Spectrochimica Acta Part A: Molecular and Biomolecular Spectroscopy 97 (2012) 167–175

Contents lists available at SciVerse ScienceDirect

Spectrochimica Acta Part A: Molecular and Biomolecular Spectroscopy

journal homepage: www.elsevier.com/locate/saa

Synthesis, spectroscopic properties and theoretical studies of bis-Schiff bases derived from polyamine and pyrazolones

Tiegang Ren [a,*], Shuyun Liu [b], Guihui Li [c], Jinglai Zhang [a], Jia Guo [a], Weijie Li [a], Lirong Yang [a]

[a] *Fine Chemistry and Engineering Research Institute, College of Chemistry and Chemical Engineering, Henan University, Kaifeng 475004, People's Republic of China*
[b] *Chemical Engineering and Technology Major, Hunan City University, Yiyang 413000, People's Republic of China*
[c] *Key Laboratory of Ministry of Education for Special Functional Materials, Henan University, Kaifeng 475004, People's Republic of China*

HIGHLIGHTS

- ▶ A series of novel Schiff bases containing pyrazole group were synthesized and characterized.
- ▶ The UV–vis spectra and fluorescent spectra of various as-synthesized products were measured.
- ▶ The B3LYP/6-31G(d) method was used for the optimization of the ground state geometry of the Schiff bases.
- ▶ The spectroscopic properties of the Schiff bases were computed based on cc-pVDZ basis set of TD-B3LYP method.

GRAPHICAL ABSTRACT

A series of novel bis-Schiff bases containing pyrazole group were synthesized using polyamine and 1-aryl-3-methyl-4-benzoyl-5-pyrazolones as the starting materials. The ultraviolet absorption and fluorescence spectra of these compounds have been studied systematically. Moreover, the B3LYP/6-31G(d) method was used to optimize the ground state geometry of the bis-Schiff bases; and the spectroscopic properties of the products were computed based on cc-pVDZ basis set of TD-B3LYP method.

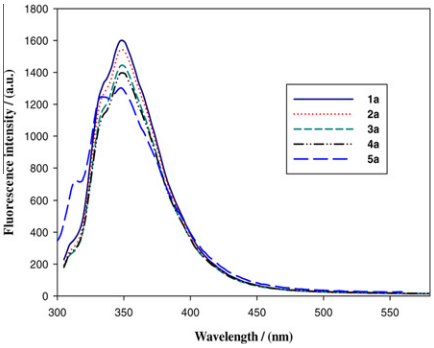

ARTICLE INFO

Article history:
Received 8 April 2012
Received in revised form 10 May 2012
Accepted 6 June 2012
Available online 13 June 2012

Keywords:
Pyrazolone
Schiff base
Polyamine
Synthesis
Spectroscopic properties
Theoretical studies

ABSTRACT

A series of novel bis-Schiff base were synthesized from 1-aryl-3-methyl-4-benzoyl-5-pyrazolones and diethylenetriamine (or triethylenetetramine) as the starting materials. All of these bis-Schiff bases were characterized by means of NMR, IR, and MS. The UV–vis absorption spectra and fluorescent spectra of these bis-Schiff bases were also measured. Moreover, the B3LYP/6-31G(d) method was used to optimize the ground state geometry of the bis-Schiff bases; and the UV–vis spectroscopic properties of the products were computed and compared with corresponding experimental data based on cc-pVDZ basis set of TD-B3LYP method. It has been found that all of these bis-Schiff bases show a remarkable absorption peak in a wavelength range of 270–340 nm; and their maximum emission peaks are around 348 nm.

Introduction

Schiff bases as important ligands in coordination chemistry can be applied in many fields [1–3]. Particularly, the Schiff base derivatives of 1-aryl-3-methyl-4-benzoyl-5-pyrazolone (AMBP)

---

* Corresponding author. Tel./fax: +86 378 2866141.
E-mail address: rtg@henu.edu.cn (T. Ren).

1386-1425/$ - see front matter © 2012 Elsevier B.V. All rights reserved.
http://dx.doi.org/10.1016/j.saa.2012.06.005

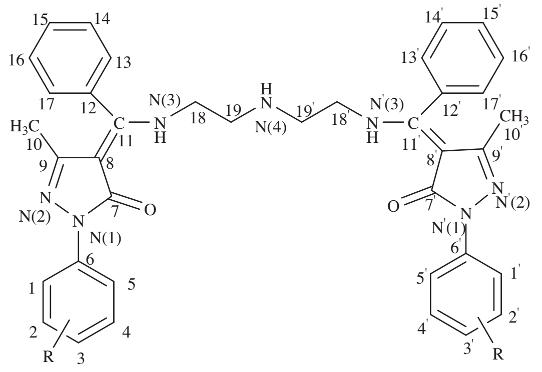

R= H (**1a**) ; *p*-CH_3 (**2a**) ; *p*-Cl (**3a**) ; *p*-Br (**4a**) ; *p*-NO_2 (**5a**)

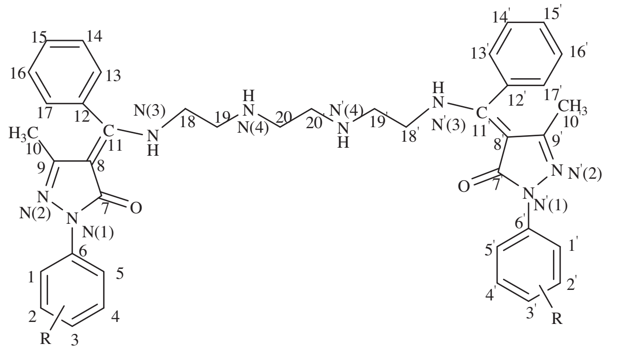

R= H (**1b**) ; *p*-CH_3 (**2b**) ; *p*-Cl (**3b**) ; *p*-Br (**4b**) ; *p*-NO_2 (**5b**) ; *m*-Cl (**6b**)

Fig. 1. The molecular structures of the Schiff base.

and their metal complexes are of extraordinary significance, since they possess high biological and pharmaceutical activities [4–7]. Similarly, polyamine derivatives (such as diethylenetriamine or triethylenetetramine [8]) as a kind of important pharmaceutical and chemical intermediates are important in enzyme catalysis, biological medicine, supramolecular self-assembly and synthesis of macrocyclic complexes, since they are closely related to cell growing development, amine nucleic acid metabolism, protein biological synthesis and sugar, lipid, and hormone metabolism [9,10]. Therefore, the Schiff base derived from polyamine and 1-phenyl-3-methyl-4-benzoyl-5-pyrazolone (PMBP) is of special interest, because it possesses unique structure and chemical properties. This is the reason why extensive researches have been focused on the synthesis and crystal structure of several Schiff bases and their metal complexes derived from diethylenetriamine and PMBP [11–16].

In our previous work, we synthesized a series of porphyrin compounds and benzimidazole compounds which contain pyrazole group, and it is found that the introduction of pyrazole group leads to stronger fluorescence emission, adding to their application as emitting materials in organic light-emitting diode (OLED), time-resolved fluoroimmunoassay and DNA probe [17,18]. Unfortunately, little is currently available about the fluorescent properties of acylpyrazolone-based Schiff bases containing different substituents in the phenyl group and the correlation between their molecular structure and emission properties, which greatly hinders their applications in biological and environmental sciences. Thus in the present research we adopt a simple procedure to synthesize bis-Schiff base compounds derived from polyamine with AMBP and investigate the correlation between their molecular structures and fluorescent properties. The equilibrium geometries and vibrational frequencies of these Schiff bases in their ground state (S_0) are

Table 1
B3LYP-optimized primary geometric parameters of the ground-state (S_0) for **1a–5a**: bond lengths (in Å), bond angles and dihedral angles (in °).

Atom numbers	Geometric parameters of S_0				
	1a	**2a**	**3a**	**4a**	**5a**
C(6)–N(1)	1.417	1.417	1.414	1.417	1.401
C(3)–*R* (*R* = CH_3, Cl, Br, NO_2)		1.510	1.756	1.915	1.451
N(1)–N(2)	1.379	1.378	1.378	1.370	1.377
C(8)–C(11)	1.469	1.471	1.471	1.487	1.494
C(11)–N(3)	1.286	1.285	1.286	1.286	1.281
N(3)–C(18)	1.455	1.452	1.453	1.454	1.451
C(19)–N(4)	1.473	1.473	1.474	1.481	1.478
C(19)′–N(4)	1.479	1.479	1.480	1.472	1.478
N(3)′–C(18)′	1.453	1.454	1.453	1.457	1.452
C(11)′–N(3)′	1.286	1.286	1.285	1.303	1.288
C(8)′–C(11)′	1.485	1.485	1.486	1.447	1.474
N(1)′–N(2)′	1.371	1.370	1.371	1.390	1.373
C(3)′–*R*′ (*R* = CH_3, Cl, Br, NO_2)		1.511	1.763	1.913	1.466
C(6)′–N(1)′	1.422	1.421	1.419	1.419	1.415
C(1)–C(6)–N(1)	120.5	120.8	120.8	121.3	120.4
C(7)–C(8)–C(11)	126.0	125.8	125.7	128.8	126.2
C(11)–N(3)–C(18)	120.9	121.9	121.5	126.7	129.2
N(3)–C(18)–C(19)	108.2	108.3	108.3	119.5	124.7
C(18)–C(19)–N(4)	111.1	111.0	111.0	110.7	113.2
C(19)–N(4)–C(19)′	113.9	114.0	114.0	113.4	111.7
C(18)′–C(19)′–N(4)	110.4	110.6	110.2	111.5	112.8
N(3)′–C(18)′–C(19)′	119.9	119.6	120.3	108.8	106.8
C(11)′–N(3)′–C(18)′	126.7	126.8	127.0	121.8	123.8
C(7)′–C(8)′–C(11)′	129.0	128.8	129.0	121.1	128.0
C(1)′–C(6)′–N(1)′	118.4	121.6	121.8	121.6	118.1
C(5)–C(6)–N(1)–N(2)	21.7	24.0	17.6	22.7	24.3
C(7)–C(8)–C(11)–C(12)	−135.1	−135.1	−134.4	−135.2	−102.3
C(8)–C(11)–C(12)–C(13)	35.7	35.2	35.4	35.2	13.6
C(11)–N(3)–C(18)–C(19)	46.9	47.5	45.6	47.9	32.7
C(11)′–N(3)′–C(18)′–C(19)′	−159.9	−152.8	−154.1	−172.3	−136.6
C(8)′–C(11)′–C(12)′–C(13)′	113.7	124.2	120.7	101.7	126.0
C(7)′–C(8)′–C(11)′–C(12)′	158.5	150.1	151.2	177.9	147.7
C(5)′–C(6)′–N(1)′–N(2)′	141.2	143.1	145.0	179.2	152.5

Table 2
B3LYP-optimized primary geometric parameters of the ground-state (S_0) for **1b**–**6b**: bond lengths (in Å), bond angles and dihedral angles (in °).

Atom numbers	Geometric parameters of S_0					
	1b	**2b**	**3b**	**4b**	**5b**	**6b**
C(6)–N(1)	1.416	1.416	1.413	1.413	1.410	1.413
C(3)–*R* (*R* = CH_3, Cl, Br, NO_2)		1.510	1.756	1.910	1.444	
C(4)–*R* (*R* = Cl)						1.757
N(1)–N(2)	1.378	1.377	1.378	1.378	1.379	1.378
C(8)–C(11)	1.474	1.486	1.475	1.475	1.475	1.475
C(11)–N(3)	1.285	1.284	1.285	1.285	1.284	1.285
N(3)–C(18)	1.452	1.450	1.452	1.452	1.452	1.452
C(19)–N(4)	1.461	1.461	1.461	1.461	1.461	1.461
C(19)′–N(4)	1.461	1.461	1.461	1.461	1.461	1.461
N(3)′–C(18)′	1.450	1.452	1.450	1.450	1.450	1.450
C(11)′–N(3)′	1.284	1.285	1.284	1.284	1.283	1.284
C(8)′–C(11)′	1.487	1.474	1.487	1.487	1.488	1.488
N(1)′–N(2)′	1.377	1.378	1.377	1.377	1.378	1.377
C(4)′–*R*′ (*R*′ = Cl)						1.756
C(3)′–*R*′ (*R*′ = CH_3, Cl, Br, NO_2)		1.510	1.756	1.909	1.444	
C(6)′–N(1)′	1.416	1.416	1.414	1.414	1.411	1.413
C(1)–C(6)–N(1)	120.6	120.7	120.9	120.9	120.7	120.9
C(7)–C(8)–C(11)	125.8	127.2	125.7	125.7	125.8	125.7
C(11)–N(3)–C(18)	122.3	121.8	117.5	122.4	122.5	122.4
N(3)–C(18)–C(19)	109.2	109.7	109.2	109.1	109.9	109.2
C(18)–C(19)–N(4)	110.5	110.5	110.5	110.6	110.6	110.5
C(19)–N(4)–C(20)	113.6	113.4	113.5	113.5	113.2	113.4
C(20)′–N(4)′–C(19)′	113.4	113.5	113.4	113.4	113.2	113.4
C(18)′–C(19)′–N(4)	110.5	110.5	110.5	110.5	110.4	110.5
N(3)′–C(18)′–C(19)′	109.7	109.2	109.7	109.7	109.7	109.7
C(11)′–N(3)′–C(18)′	121.8	122.3	121.9	121.9	122.1	121.9
C(7)′–C(8)′–C(11)′	127.1	125.8	127.1	127.1	127.2	127.0
C(1)′–C(6)′–N(1)′	120.4	119.5	120.8	120.8	120.6	120.7
C(5)–C(6)–N(1)–N(2)	−34.9	−35.4	−33.4	−33.3	−30.7	−32.7
C(7)–C(8)–C(11)–C(12)	−148.3	−148.5	−148.0	−148.0	−150.0	−147.9
C(8)–C(11)–C(12)–C(13)	55.8	55.9	55.5	55.4	60.0	55.0
C(11)–N(3)–C(18)–C(19)	138.0	138.0	138.1	138.0	122.7	138.8
N(4)–C(20)–C(20)′–N(4)′	−179.7	−179.7	−179.8	−179.9	−179.8	−179.6
C(11)′–N(3)′–C(18)′–C(19)′	151.1	151.1	150.5	150.5	150.3	150.9
C(8)′–C(11)′–C(12)′–C(13)′	21.5	21.6	21.2	21.3	21.8	20.4
C(7)′–C(8)′–C(11)′–C(12)′	−123.7	−123.9	−123.1	−123.2	−122.9	−122.6
C(5)′–C(6)′–N(1)′–N(2)′	144.2	143.2	145.9	146.0	148.8	146.7

determined using the B3LYP method with 6-31G(d) basis set, and their absorption spectra are theoretically calculated using the TD-B3LYP method with cc-pVDZ basis set and compared to the experimental ones.

Experimental

Physical measurement and materials

Infrared (IR) spectra of these products were recorded with a Nicolet 170 SXFT-IR spectrometer within 400–4000 cm^{-1} (mixed with KBr and pressed into pellets). Mass spectra (MS) were determined with an Agilent 1100LC-MS mass spectrometer. Nuclear magnetic resonance (^1H NMR and ^{13}C NMR) spectra were recorded with an INOVA-400 spectrometer in $CDCl_3$ or dimethyl sulphoxide (DMSO) using tetramethyl silane (TMS) as an internal standard. The fluorescence behavior at room temperature was evaluated using a Hitachi F-7000 facility (light source: Xe arc lamp). Ultraviolet–visible light (UV–vis) absorption spectra were measured with a Hitachi U-4100 spectrophotometer. The equilibrium geometries and vibrational frequencies of as-synthesized products in their ground-state were determined by B3LYP method with the 6-31G(d) basis set, and their absorption spectra were estimated using the TD-B3LYP method and cc-pVDZ basis set [19], and all of the calculations were performed in vacuum. All the reagents were purchased from commercial sources (AR grade); and solvents used in this study were purified following the standard procedures.

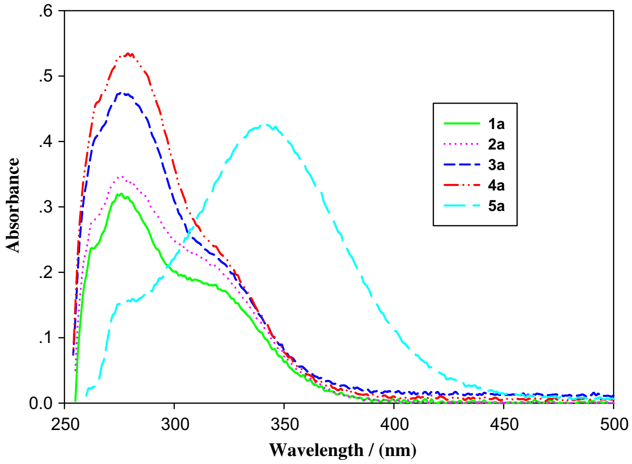

Fig. 2. UV–Vis Absorption spectra of **1a**–**5a**.

General procedure for the preparation of Schiff base

1-aryl-3-methyl-4-benzoyl-5-pyrazolones were prepared according to published procedure [20]. Known structures of synthesized products were verified by comparing their data with those reported in the literature. Briefly, a certain amount of 1-aryl-3-methyl-4-benzoyl-5-pyrazolones (4 mmol) was dissolved in 50 mL ethanol, followed by dropwise addition of ethanol containing an appropriate

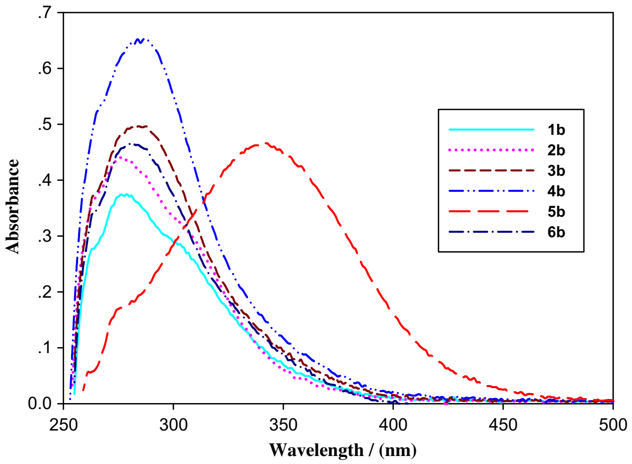

Fig. 3. UV–Vis Absorption spectra of **1b**–**6b**.

Table 3
The calculated absorption wavelengths of **1a**–**5a** at the TD-B3LYP/cc-pVDZ level.

Compounds	States	Transition	Absorption	
			λ	f
1a	X^1A	$(164a)^2(165a)^2(166a)^0$		
	12^1A	161a → 166a	266.34 (276.8)[a]	0.2241
	26^1A	160a → 167a	247.15	0.2936
2a	X^1A	$(172a)^2(173a)^2(174a)^0$		
	10^1A	169a → 174a	275.04 (275.4)[a]	0.1629
	20^1A	173a → 179a	255.93	0.2865
3a	X^1A	$(180a)^2(181a)^2(182a)^0$		
	10^1A	177a → 182a	275.50(276.0)[a]	0.1665
	22^1A	177a → 185a	253.29	0.2369
4a	X^1A	$(198a)^2(199a)^2(200a)^0$		
	3^1A	199a → 200a	297.84	0.2201
	6^1A	198a → 201a	282.36 (278.2)[a]	0.1925
	24^1A	194a → 201a	251.38	0.1607
5a	X^1A	$(186a)^2(187a)^2(188a)^0$		
	5^1A	184a → 188a	384.65	0.1833
	11^1A	187a → 189a	337.76 (340.0)[a]	0.2719

[a] Experimental values in DMF solution.

Table 4
The calculated absorption wavelengths of **1b**–**6b** at the TD-B3LYP/cc-pVDZ level.

Compounds	States	Transition	Absorption	
			λ	f
1b	X^1A	$(176a)^2(177a)^2(178a)^0$		
	14^1A	173a → 179a	268.90 (276.8)[a]	0.1428
2b	X^1A	$(184a)^2(185a)^2(186a)^0$		
	12^1A	182a → 187a	272.15 (276.0)[a]	0.1303
	30^1A	182a → 191a	252.39	0.3179
3b	X^1A	$(192a)^2(193a)^2(194a)^0$		
	21^1A	189a → 195a	270.40 (284.0)[a]	0.2680
	31^1A	184a → 194a	255.62	0.1769
4b	X^1A	$(210a)^2(211a)^2(212a)^0$		
	20^1A	208a → 213a	271.64 (287.0)[a]	0.3036
	31^1A	204a → 212a	256.19	0.2207
5b	X^1A	$(198a)^2(199a)^2(200a)^0$		
	9^1A	195a → 201a	303.48 (340.6)[a]	0.3081
	24^1A	191a → 200a	277.05	0.1631
6b	X^1A	$192a)^2(193a)^2(194a)^0$		
	24^1A	187a → 194a	265.61 (281.0)[a]	0.2291
	31^1A	186a → 194a	254.59	0.1345

[a] Experimental values in DMF solution.

amount of amine (4 mmol of diethylenetriamine (DETA) or triethylenetetramine (TETA)). Resultant mixture was refluxed in a water bath for 4 h before rotary evaporating to remove solvent and cooling to room temperature. As-separated yellow crystalline precipitates were collected by filtration and recrystallized with ethanol-chloroform (1:3, V/V).

(4Z,4′Z)-4,4′-(2,2′-azanediylbis(ethane-2,1-diyl)bis(azanediyl))-bis(phenylmethan-1-yl-1-ylidene)bis(3-methyl-1-phenyl-1H-pyrazol-5(4H)-one) (**1a**). APCI-MS (m/z) calcd (M^+): 624.8, found: 624.0; IR (KBr, cm^{-1}): 1627 ($\nu_{C=N}$), 1151 (ν_{C-O}), 1537, 1498 ($\nu_{C=C}$), 3058 ($\nu_{N-H\cdots O}$); ^1H NMR ($CDCl_3$) δ: 1.34 (s, 6H, $2CH_3$), 1.6 (b, 1H, NH), 2.79 (t, 4H, J = 2.8 Hz, CH_2–CH_2), 3.2 (dd, 4H, J = 5.6, 5.6 Hz, CH_2–CH_2), 7.12 (t, 2H, J = 7.1 Hz, Ar–H), 7.36–7.39 (m, 8H, Ar–H), 7.49 (t, 6H, J = 7.5 Hz, Ar–H), 7.99 (d, 4H, J = 8.0 Hz, Ar–H), 11.30 (s, 2H, NH). ^{13}C NMR ($CDCl_3$) δ: 166.07, 165.74, 147.97, 139.23, 131.49, 130.50, 129.11, 128.72, 127.59, 124.24, 119.40, 99.80, 48.50, 44.46, 15.40.

(4Z,4′Z)-4,4′-(2,2′-azanediylbis(ethane-2,1-diyl)bis(azanediyl)) bis(phenylmethan-1-yl-1-ylidene)bis(3-methyl-1-*p*-tolyl-1H-pyrazol-5(4H)-one) (2a). APCI-MS (m/z) calcd (M^+): 652.8, found: 651.2; IR (KBr, cm^{-1}): 1630 ($\nu_{C=N}$), 1156 (ν_{C-O}), 1536, 1479 ($\nu_{C=C}$), 3038 ($\nu_{N-H\cdots O}$); ^1H NMR ($CDCl_3$) δ: 1.37 (s, 6H, $2CH_3$), 2.34 (s, 6H, $2CH_3$), 2.79 (t, 4H, J = 2.8 Hz, CH_2–CH_2), 3.2 (dd, 4H, J = 5.6, 3.6 Hz, CH_2–CH_2), 7.17 (d, 4H, J = 8.4 Hz, Ar–H), 7.34 (dd, 4H, J = 3.6, 1.6 Hz, Ar–H), 7.51 (t, 6H, J = 7.5 Hz, Ar–H), 7.85 (d, 4H, J = 8.4 Hz, Ar–H), 11.31 (s, 2H, NH). ^{13}C NMR ($CDCl_3$) δ: 165.96, 165.58, 147.69, 136.82, 133.77, 131.51, 130.40, 129.27, 129.13, 127.59, 119.39, 99.87, 48.65, 44.46, 21.08, 15.54.

(4Z,4′Z)-4,4′-(2,2′-azanediylbis(ethane-2,1-diyl)bis(azanediyl)) bis(phenylmethan-1-yl-1-ylidene)bis(1-(4-chlorophenyl)-3-methyl-1H-pyrazol-5(4H)-one) (**3a**). APCI-MS (m/z) calcd (M^+): 693.6, found: 693.2; IR (KBr, cm^{-1}): 1626 ($\nu_{C=N}$), 1159 (ν_{C-O}), 1536, 1492 ($\nu_{C=C}$), 3066 ($\nu_{N-H\cdots O}$); ^1H NMR ($CDCl_3$) δ: 1.29 (s, 6H, $2CH_3$), 1.46 (b, 1H, NH), 2.81 (t, 4H, J = 2.8 Hz, CH_2–CH_2), 3.2 (dd, 4H, J = 5.6, 5.6 Hz, CH_2–CH_2), 7.31 (d, 4H, J = 8.8 Hz, Ar–H), 7.37–7.40 (m, 4H, Ar–H), 7.48–7.54 (m, 6H, Ar–H), 7.98 (d, 4H, J = 8.8 Hz, Ar–H), 11.24 (s, 2H, NH). ^{13}C NMR ($CDCl_3$) δ: 166.18, 165.68, 148.26, 137.89, 131.39, 130.49, 129.11, 128.98, 128.65, 127.54, 120.21, 99.65, 48.28, 44.38, 15.36.

(4Z,4′Z)-4,4′-(2,2′-azanediylbis(ethane-2,1-diyl)bis(azanediyl)) bis(phenylmethan-1-yl-1-ylidene)bis(1-(4-bromophenyl)-3-methyl-1H-pyrazol-5(4H)-one) (**4a**). APCI-MS (m/z) calcd (M^+): 782.5, found: 782.1; IR (KBr, cm^{-1}): 1626 ($\nu_{C=N}$), 1158 (ν_{C-O}), 1536, 1490 ($\nu_{C=C}$), 3063 ($\nu_{N-H\cdots O}$); ^1H NMR ($CDCl_3$) δ: 1.29 (s, 6H, $2CH_3$), 1.71 (b, 1H, NH), 2.81 (t, 4H, J = 2.8 Hz, CH_2–CH_2), 3.2 (dd, 4H, J = 5.6, 5.6 Hz, CH_2–CH_2), 7.37–7.40 (m, 4H, Ar–H), 7.45–7.53 (m, 10H, Ar–H), 7.93 (d, 4H, J = 8.8 Hz, Ar–H), 11.23 (s, 2H, NH). ^{13}C NMR ($CDCl_3$) δ: 165.15, 165.69, 148.28, 138.36, 131.54, 131.35, 130.48, 129.09, 127.51, 120.49, 116.71, 99.64, 48.26, 44.37, 15.35.

(4Z,4′Z)-4,4′-(2,2′-azanediylbis(ethane-2,1-diyl)bis(azanediyl)) bis(phenylmethan-1-yl-1-ylidene)bis(3-methyl-1-(4-nitrophenyl) -1H-pyrazol-5(4H)-one) (**5a**). APCI-MS (m/z) calcd (M^+): 714.7, found: 714.4; IR (KBr, cm^{-1}): 1636 ($\nu_{C=N}$), 1158 (ν_{C-O}), 1539, 1496 ($\nu_{C=C}$), 3197 ($\nu_{N-H\cdots O}$); ^1H NMR ($CDCl_3$) δ: 1.21 (s, 6H, $2CH_3$), 2.12 (b, 1H, NH), 2.87 (t, 4H, J = 2.9 Hz, CH_2–CH_2), 3.25 (m, 4H, CH_2–CH_2), 7.43–7.46 (m, 4H, Ar–H), 7.54–7.57 (m, 6H, Ar–H), 8.19–8.26 (m, 8H, Ar–H), 11.23 (s, 2H, NH). ^{13}C NMR ($CDCl_3$) δ: 166.58, 149.83, 144.51, 142.99, 131.29, 130.75, 129.22, 127.54, 124.75, 117.75, 99.46, 53.59, 47.95, 44.44, 15.39.

(4Z,4′Z)-4,4′-(1,12-diphenyl-2,5,8,11-tetraazadodecane-1,12-diylidene)bis(3-methyl-1-phenyl-1H-pyrazol-5(4H)-one) (**1b**). APCI-MS (m/z) calcd (M^+): 667.8, found: 667.4; IR (KBr, cm^{-1}): 1629 ($\nu_{C=N}$), 1151 (ν_{C-O}), 1536, 1499 ($\nu_{C=C}$), 3059 ($\nu_{N-H\cdots O}$); ^1H NMR ($CDCl_3$) δ: 1.41 (d, 6H, J = 16 Hz, $2CH_3$), 1.80 (b, 1H, NH), 2.44 (s, 2H, CH_2), 2.55 (b, 1H, NH), 2.74–2.84 (m, 6H, $3CH_2$), 3.21 (s, 4H, CH_2–CH_2), 7.12 (t, 2H, J = 7.1 Hz, Ar–H), 7.22 (d, 2H, J = 7.2 Hz, Ar–H), 7.35–7.48 (m, 10H, Ar–H), 7.54 (s, 2H, Ar–H), 8.02 (t, 4H, J = 8.0 Hz, Ar–H), 11.26 (d, 2H, NH). ^{13}C NMR ($CDCl_3$)

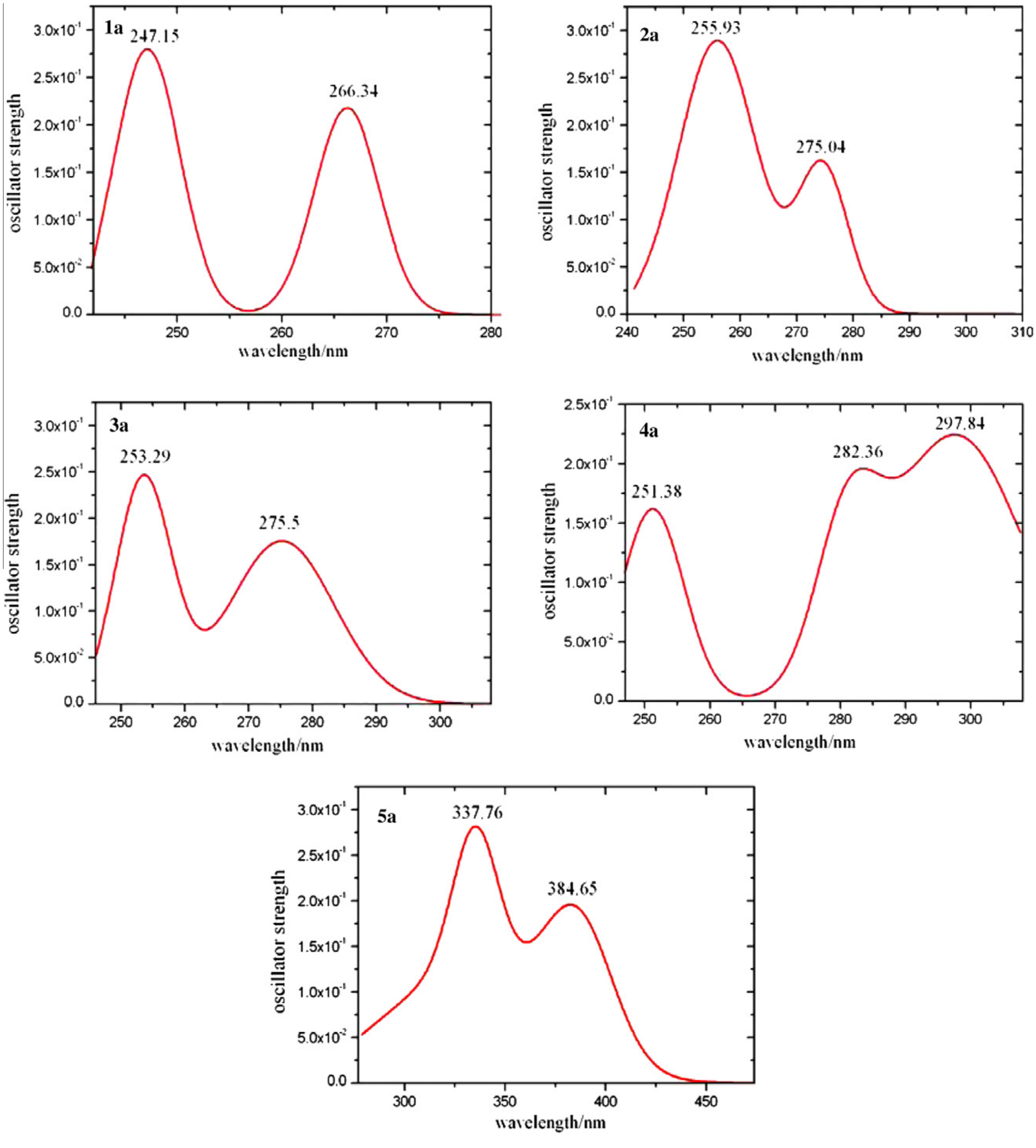

Fig. 4. Theoretical absorption spectra of **1a**–**5a**.

δ: 165.58, 147.97, 139.37, 131.57, 130.20, 129.00, 128.69, 127.33, 124.16, 119.12, 99.56, 53.00, 48.48, 44.06, 41.72, 15.42.

(4Z,4′Z)-4,4′-(1,12-diphenyl-2,5,8,11-tetraazadodecane-1,12-diylidene)bis(3-methyl-1-*p*-tolyl-1H-pyrazol-5(4H)-one) (**2b**). APCI-MS (m/z) calcd (M^+): 695.8, found: 695.5; IR (KBr, cm^{-1}): 1631 ($\nu_{C{=}N}$), 1153 ($\nu_{C{-}O}$), 1535, 1479 ($\nu_{C{=}C}$), 3452 ($\nu_{N{-}H\cdots O}$); ^1H NMR ($CDCl_3$) δ: 1.41 (d, 6H, J = 14.0 Hz, $2CH_3$), 1.82 (b, 1H, NH), 2.32 (d, 6H, J = 8.0 Hz, $2CH_3$), 2.42 (s, 2H, CH_2), 2.54 (t, 1H, J = 2.5 Hz, NH), 2.74–2.84 (m, 6H, $3CH_2$), 3.18 (m, 4H, CH_2–CH_2), 7.16–7.34 (m, 8H, Ar–H), 7.40–7.54 (m, 6H, Ar–H), 7.88 (t, 4H, J = 8.9 Hz, Ar–H), 11.26 (d, 2H, NH). ^{13}C NMR ($CDCl_3$) δ: 165.57, 147.71, 137.02, 133.64, 131.73, 130.23, 129.30, 129.05, 127.42, 119.24, 99.69, 53.10, 48.62, 44.10, 41.79, 21.05, 15.48.

(4Z,4′Z)-4,4′-(1,12-diphenyl-2,5,8,11-tetraazadodecane-1,12-diylidene)bis(1-(4-chlorophenyl) -3-methyl-1H-pyrazol-5(4H)-one) (**3b**). APCI-MS (m/z) calcd (M^+): 736.7, found: 735.3; IR (KBr, cm^{-1}): 1636 ($\nu_{C{=}N}$), 1152 ($\nu_{C{-}O}$), 1536, 1490 ($\nu_{C{=}C}$), 3065 ($\nu_{N{-}H\cdots O}$); ^1H NMR ($CDCl_3$) δ: 1.39 (d, 6H, J = 16.8 Hz, $2CH_3$), 2.46–2.58 (m, 8H, $2CH_2$–CH_2), 2.79 (s, 1H, NH), 2.85 (t, 1H, J = 2.9 Hz, NH), 3.21–3.25 (m, 4H, CH_2–CH_2), 7.21 (d, 2H, J = 6.8 Hz, Ar–H), 7.27–7.35 (m, 6H, Ar–H), 7.43–7.56 (m, 6H, Ar–H), 7.99 (d, 4H, J = 9.2 Hz, Ar–H), 11.21 (d, 2H, NH). ^{13}C NMR

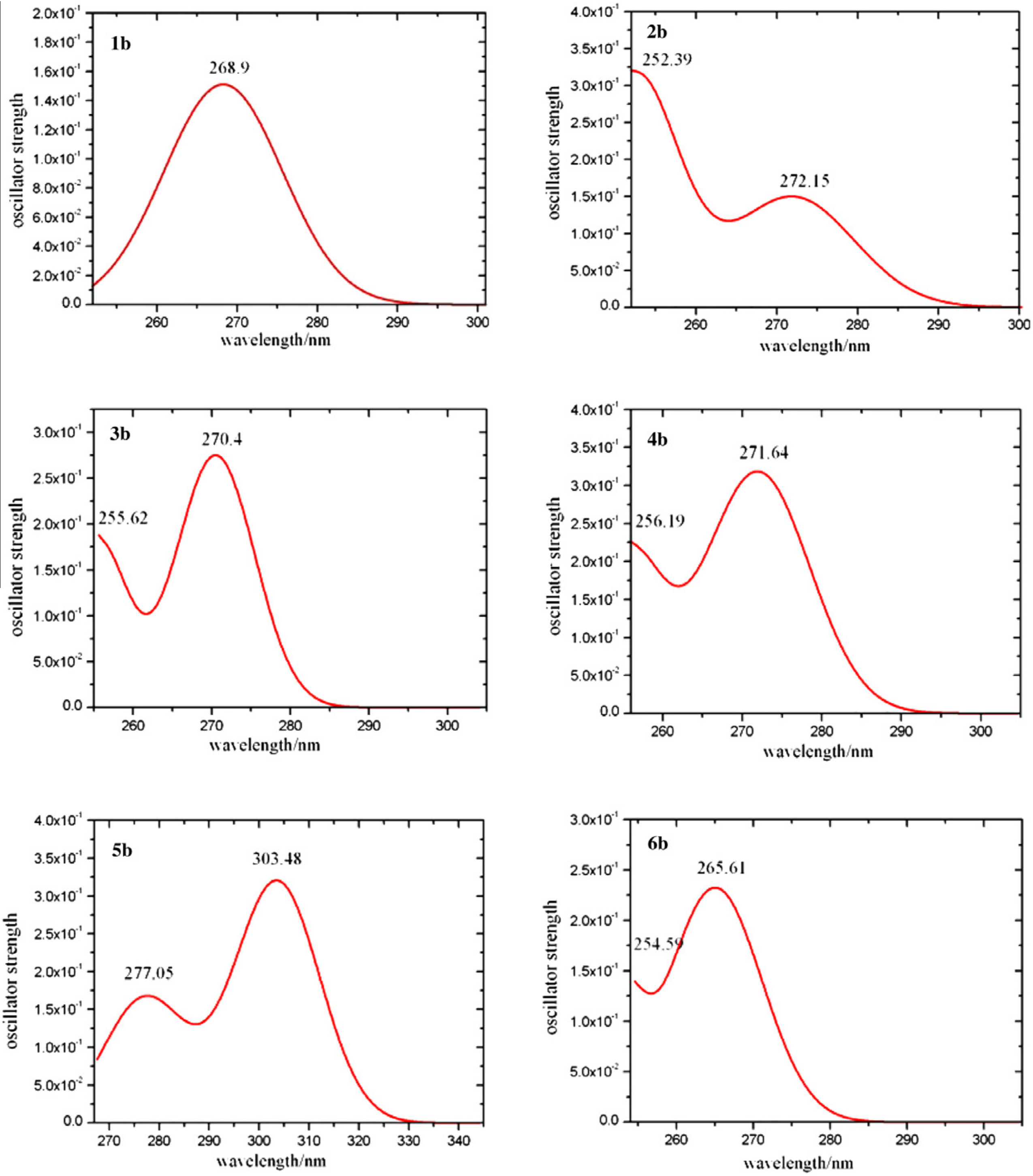

Fig. 5. Theoretical absorption spectra of **1b**–**6b**.

($CDCl_3$) δ: 165.81, 165.69, 148.26, 137.97, 131.57, 130.54, 129.21, 128.78, 127.38, 120.16, 99.73, 57.45, 53.08, 48.45, 41.83, 15.51.

(4Z,4′Z)-4,4′-(1,12-diphenyl-2,5,8,11-tetraazadodecane-1,12-diylidene)bis(1-(4-bromophenyl) -3-methyl-1H-pyrazol-5(4H)-one) (**4b**). APCI-MS (m/z) calcd (M^+): 835.6, found: 825.3; IR (KBr, cm^{-1}): 1636 ($\nu_{C=N}$), 1152 ($\nu_{C–O}$), 1536, 1488 ($\nu_{C=C}$), 3048 ($\nu_{N–H\cdots O}$); ^1H NMR ($CDCl_3$) δ: 1.39 (d, 6H, J = 17.2 Hz, $2CH_3$), 2.46–2.57 (m, 8H, $2CH_2–CH_2$), 2.79 (s, 1H, NH), 2.85 (t, 1H, J = 2.9 Hz, NH), 3.20–3.24 (m, 4H, $CH_2–CH_2$), 7.20 (d, 2H, J = 7.2 Hz, Ar–H), 7.32–7.34 (m, 2H, Ar–H), 7.43–7.56 (m, 10H, Ar–H), 7.95 (d, 4H, J = 8.8 Hz, Ar–H), 11.20 (d, 2H, NH). ^{13}C NMR ($CDCl_3$) δ: 165.78, 165.69, 148.29, 137.94, 131.53, 130.54, 129.22, 128.79, 127.36, 120.14, 99.71, 57.44, 53.07, 48.34, 41.80, 15.54.

(4Z,4′Z)-4,4′-(1,12-diphenyl-2,5,8,11-tetraazadodecane-1,12-diylidene)bis(3-methyl-1-(4-nitrophenyl)-1H-pyrazol-5(4H)-one) (**5b**). APCI-MS (m/z) calcd (M^+): 758.8, found: 757.4; IR (KBr, cm^{-1}): 1638 ($\nu_{C=N}$), 1153 ($\nu_{C–O}$), 1540, 1499 ($\nu_{C=C}$), 3068 ($\nu_{N–H\cdots O}$); ^1H NMR ($CDCl_3$) δ: 1.40 (s, 6H, $2CH_3$), 2.11 (b, 1H, NH), 2.55 (m, 1H, NH), 2.83–2.91 (m, 8H, $2CH_2–CH_2$), 3.24–3.28 (m, 4H, CH_2–CH_2), 7.24 (d, 2H, *J* = 8.0 Hz, Ar–H), 7.34–7.59 (m, 8H, Ar–H), 8.21–8.30 (m, 8H, Ar–H), 7.95 (d, 4H, *J* = 8.8 Hz, Ar–H), 11.28 (d, 2H, NH). ^{13}C NMR ($CDCl_3$) δ: 165.84, 148.45, 138.54, 131.67, 131.51, 130.44, 129.15, 127.30, 120.47, 116.76, 99.59, 57.43, 53.07, 48.42, 44.03, 15.49.

(4Z,4′Z)-4,4′-(1,12-diphenyl-2,5,8,11-tetraazadodecane-1,12-diylidene)bis(1-(3-chlorophenyl)-3-methyl-1H-pyrazol-5(4H)-one) (**6b**). APCI-MS (m/z) calcd (M^+): 736.7, found: 735.3; IR (KBr, cm^{-1}): 1637($\nu_{C=N}$), 1151 ($\nu_{C–O}$), 1540, 1478 ($\nu_{C=C}$), 3058 ($\nu_{N–H\cdots O}$); ^{1}H NMR ($CDCl_3$) δ: 1.39 (d, 6H, *J* = 18.8 Hz, $2CH_3$), 2.47–2.58 (m, 8H, $2CH_2$–CH_2), 2.78 (s, 1H, NH), 2.56 (t, 1H, *J* = 2.6 Hz, NH), 3.21–3.25 (m, 4H, CH_2–CH_2), 7.08 (t, 2H, *J* = 7.1 Hz, Ar–H), 7.23 (d, 2H, *J* = 8.0 Hz, Ar–H), 7.30–7.34 (m, 4H, Ar–H), 7.42–7.55 (m, 6H, Ar–H), 7.97 (t, 2H, *J* = 7.9 Hz, Ar–H), 8.11 (d, 2H, *J* = 10.0 Hz, Ar–H), 11.21 (d, 2H, NH). ^{13}C NMR ($CDCl_3$) δ: 165.72, 148.47, 140.38, 134.45, 131.50, 130.55, 129.84, 129.27, 127.37, 124.01, 118.88, 116.80, 99.70, 57.43, 53.06, 44.11, 41.80, 15.54.

Results and discussion

Synthesis

In our previous paper [21], a series of benzimidazoles were obtained from 1-arylpyrazole-4-carbaldehyde and *o*-phenylenediamine, where mono-Schiff base was obtained as an unstable intermediate which was eventually transformed to benzimidazoles. However, when we used 1-aryl-3-methyl-4-benzoyl-5-pyrazolones to replace 1-arylpyrazole-4-carbaldehyde and react with phenylenediamine, only mono-Schiff bases were obtained, possibly because the benzene ring connected with the carbonyl group possesses a stronger steric hindrance effect than the H atom connected with the carbonyl and the two $-NH_2$ radicals in phenylenediamine molecules are too short. Thus we selected longer polyamines such as diethylenetriamine and triethylenetetramine to condense with 1-aryl-3-methyl-4-benzoyl-5-pyrazolones so as to yield bis-Schiff bases with salen-like configuration [22,23]. Similarly, Fredy et al. [15] and Fabio et al. [16] separately synthesized some bis-Schiff bases from pyrazolone and some diamines, which, we suppose, might be related to the large steric hindrance for the connection of phenyl group with carbonyl. Moreover, we also found that the substituent *R* on the phenyl group of pyrazolone had a significant influence on the yield of Schiff bases target products and relevant intermediates. For example, when pyrazolones containing phenyl group with electron withdrawing substituents such as F, Cl, Br and $-NO_2$ were used, target products 1-aryl-3-methyl-5-pyrazolones were obtained without adjusting pH = 7.0 in a higher yield as compared with the pyrazolones containing phenyl group with electron donating substituents.

Ground-state geometries at the B3LYP level

The molecular structures of the two series of Schiff base are depicted in Fig. 1, and the B3LYP-optimized primary geometric parameters (bond lengths, bond angles, and dihedral angles) of ground state (S_0) are summarized in Tables 1 and 2.

As it can be seen in Fig. 1 and Table 1, the five **a**-series compounds, except for **4a**, have the same matrix of **1a** and possess very similar S_0 geometric parameters (bond lengths and bond angles). Compound **4a** has better coplanarity than the other **a**-series compounds, showing dihedral angles of −172.3°, 101.7°, 177.9° and 179.2°for C(11)′–N(3)′–C(18)′–C(19)′, C(8)′–C(11)′–C(12)′–C(13)′, C(7)′–C(8)′–C(11)′–C(12)′, and C(5)′–C(6)′–N(1)′–N(2)′. Similarly, the ground-state geometric parameters of compounds **1a**–**5a** (bond lengths and bond angles) are very similar.

The primary geometric parameters of 1b–6b are shown in Table 2. In combination with the data listed in Table 2, it can be seen that their ground-state (S_0) geometric parameters, bond lengths, bond angles, and dihedral angles are very similar.

In addition, vibrational frequency analyses based upon B3LYP/6-31G(d) calculations reveal that the two series of Schiff base have stable structures on the potential energy surfaces, showing no imaginary frequency.

UV–vis spectra

Figs. 2 and 3 show the UV–vis spectra of the two series of as-synthesized Schiff bases measured in dimethyl formamide (DMF). In the exploited wavelength region (200–800 nm), all as-synthesized Schiff bases show a remarkable absorption peak at 270–340 nm, which is attributed to the $\pi \rightarrow \pi^*$ transition and $n \rightarrow \pi^*$ transition. In the meantime, substituent *R* of the phenyl group has significant influence on the absorption wavelength and absorbance. On the one hand, the introduction of auxochrome group such as F, Cl, Br and NO_2 to the phenyl group allows conjugation of nonbonding electron with π electron to form p–π conjugation, leading to enhanced electronic scope of operation and shift of absorption peak towards longer wavelength. Among the auxochrome group substituent, NO_2 as a stronger electron withdrawing group and chromophore leads to shift of the absorption peak towards longer wavelength. On the other hand, the introduction of alkyl group to the conjugated systems allows the electron of C–H bond of the alkyl group to overlap with the π electron of the conjugated system (the so-called hyperconjugation), but the influence on the absorption wavelength and absorbance is very small.

Theoretical absorption spectra at the B3LYP level

The absorption wavelengths (λ in nm) and oscillator strengths (*f*) of the two series of Schiff base which are computed using the TD-B3LYP method with the cc-pVDZ basis set [19] are listed in Tables 3 and 4, together with the experimental values. Figs. 4 and 5 illustrate the UV–vis spectra of the Schiff bases measured in DMF. By comparing with the experimental values in DMF solution, we can see that theoretical absorption spectra values agree well with the experimental ones. Each of compounds **1a**–**5a** has a main absorption peak within 270–340 nm, which is attributed to the $\pi \rightarrow \pi^*$ transition. Besides, theoretical calculations give two main absorption peaks within 240–390 nm attributed to the $\pi \rightarrow \pi^*$ transition and $n \rightarrow \pi^*$ transition (Table 3); and the theoretical absorption spectra basically agree well with relevant experimental results. For example, as shown in Table 3, compound **2a** has a ground state of singlet X^1A with an electronic configuration of $(172a)^2(173a)^2(174a)^0$ and 10^1A excited state derived from 169a → 174a orbitals, while its absorption wavelength 275.04 nm corresponding to the largest *f* of 0.1629 is in good agreement with the experimental value of 275.4 nm. Nevertheless, no absorptions are experimentally observed in relation to the calculated electron excitation of 173a → 179a leading to 20^1A state at 255.93 nm with *f* = 0.2865; and the reasons accounting for this disagreement remain unknown. Moreover, compounds **1a**–**4a** (except for **5a**) with similar charge conjugation all have the main calculated absorption wavelength of 276 nm, which indicates that the substituent *R* of their phenyl group has little influence on the absorption wavelength and absorbance. Similarly, the experimentally measured absorption wavelengths of compounds **1b**–**6b** also agree well with the theoretically calculated ones, and the theoretical calculations give more absorptions than the experimental measurements do (see Fig. 5 and Table 4). Besides, all **b**-series compounds (except for **5b**) have the main calculated absorption wavelength of 281 nm, due to their similar charge conjugation (Fig. 5).

By summarizing the data shown in Figs. 4 and 5 as well as in Tables 3 and 4, we can find that the introduction of auxochrome group like F, Cl, Br and NO_2 allows nonbonding electrons to conjugate with π electrons forming p–π conjugation. As a result, the electronic scope of operation is enhanced, and the absorption is shifted towards longer wavelength. Since auxochrome group NO_2 has stronger ability to facilitate the above-mentioned p–π conjugation than F, Cl and Br, as-synthesized Schiff bases with NO_2 substitutuent in the phenyl group have a longer UV–vis absorption wavelength.

Fluorescent spectra

The fluorescence spectra of these Schiff bases measured at room temperature in DMF are shown in Figs. 6 and 7; and their maximum absorption and maximum emission wavelengths data are listed in Tables 5 and 6. Compounds **1a**–**5a** and **1b**–**6b** excited at 295 nm in DMF solution show the maximum emission peak around 348 nm (Tables 5 and 6). This implies that the substituent *R* of the phenyl group has a minor influence on the fluorescence wavelength but a significant influence on the fluorescence intensity of these Schiff bases. Namely, electron withdrawing substituents such as *p*-Cl and *p*-F cause a slight red-shift of the fluorescent spectra and an increase of the fluorescence intensity, while electron donating substituent like *p*-CH_3 reduces the fluorescence intensity. Specifically, the increase of the polyamine chain has a minor influence on the fluorescence wavelength and intensity of these Schiff bases (Tables 5 and 6), which may be largely due to the increase of the conjugated system and the decrease of the molecular planarity.

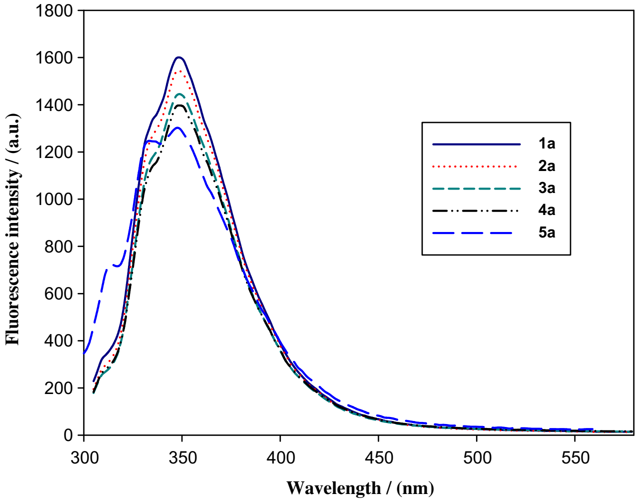

Fig. 6. The emission spectra of **1a**–**5a**.

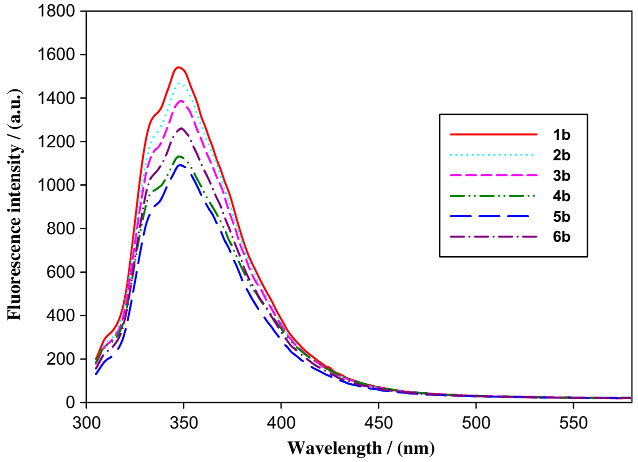

Fig. 7. The emission spectra of **1b**–**6b**.

Table 5
The maximum absorption and maximum emission wavelengths data of compounds **1a**–**5a**.

Compounds	$\lambda_{UV.max}$ (nm)	$\lambda_{FL.max}$ (nm)
1a	276.8	347.4
2a	275.4	348.6
3a	276.0	348.2
4a	278.2	349.4
5a	340.0	348.2

Table 6
The maximum absorption and maximum emission wavelengths data of compounds **1b**–**6b**.

Compounds	$\lambda_{UV.max}$ (nm)	$\lambda_{FL.max}$ (nm)
1b	276.8	348.2
2b	276.0	348.6
3b	284.0	348.6
4b	287.0	348.6
5b	340.6	347.8
6b	281.0	349.0

Conclusions

In summary, two series of novel bis-Schiff base have been successfully synthesized using 1-aryl-3-methyl-4-benzoyl-5-pyrazolones and various polyamines as the starting materials. UV–vis absorption spectra and fluorescent spectra of these Schiff bases have been measured. The equilibrium geometries and vibrational frequencies of the two series of bis-Schiff base in their ground state have been determined by B3LYP method with the 6-31G(d) basis set, and their absorption spectra have been estimated using the TD-B3LYP method and cc-pVDZ basis set. It has been found that all of these bis-Schiff bases show a noticeable absorption peak within 270–340 nm and a maximum emission peak around 348 nm. The fluorescent properties of the Schiff bases are closely related to their molecular structure.

Acknowledgements

The authors gratefully thank the Science and Technology Department of Hunan province (Project of Science and Technology Promotion Plan, Grant No. 2011FJ4169) and the Education Department of Hunan Province (Science Research Project, Grant No. 10C0499) for financial support.

References

[1] F.L. Hu, X.H. Yin, Y. Mi, S.S. Zhang, W.Q. Luo, Spectrochim. Acta A 75 (2010) 825–829.
[2] S. Banthia, A. Samanta, J. Phys. Chem. B 110 (2006) 6437–6440.
[3] S.J. Toal, K.A. Jones, D. Magde, W.C. Trogler, J. Am. Chem. Soc. 127 (2005) 11661–11665.
[4] E.C. Okafor, B.A. Uzoukwu, Radiochim. Acta 51 (1990) 167–172.
[5] A. Tong, Y. Akama, S.J. Tanaka, Chromatography 478 (1989) 408–414.
[6] L. Yand, W.Z. Jin, J. Lin, Polyhedron 19 (2000) 93–98.
[7] X.S. Fan, X.Y. Zhang, L.H. Zhou, K.A. Keith, E.R. Kern, P.F. Torrence, Bioorg. Med. Chem. Lett. 16 (2006) 3224–3228.
[8] F.R. Xiao, L. Chen, J.D. Wang, R.L. Wu, F. Yue, J. Li, Acta Chim. Sinica 64 (2006) 1517–1522.
[9] S.H. Wan, F. Liang, X.Q. Xiong, et al., Bioorg. Med. Chem. 16 (2006) 2804–2806.

[10] R. Khan, L. Gropen, P.A. Konowicz, M. Matulovà, S. Paoletti, Tetrahedron Lett. 48 (2007) 7767–7770.
[11] R.N. Jadeja, J.R. Shah, Polyhedron 26 (2007) 1677–1685.
[12] Y. Wang, Z.Y. Yang, Transition Met. Chem. 30 (2005) 902–906.
[13] Y. Wang, Z.Y. Yang, J. Lumin. 128 (2008) 373–376.
[14] L. Zhang, L. Liu, G.F. Liu, G.C. Xu, D.Z. Jia, J.P. Lang, J. Chem. Crystallogr. 35 (2005) 583–588.
[15] R. Fredy, J.B. Pérez, M. Yanko, R. Baggio, O. Peña, New J. Chem. 29 (2005) 283–287.
[16] M. Fabio, P. Claudio, P. Riccardo, A. Cingolani, D. Leonesi, A. Lorenzotti, Polyhedron 18 (1999) 3041–3050.
[17] G.F. Liu, L. Liu, D.Z. Jia, K.B. Yu, Chin. Chem. Lett. 14 (2003) 1230–1232.
[18] M.M. Mojtahedi, M. Javadpour, M.S. Abaee, Ultrason. Sonochem. 15 (2008) 828–832.
[19] P.V. Yurenev, A.V. Shcherbinin, N.F. Stepanov, Russ. J. Phys. Chem. A 84 (2010) 39–43.
[20] B.S. Jensen, Acta Chem. Scand. 13 (1959) 1668–1670.
[21] T.G. Ren, H.B. Cheng, J.L. Zhang, W.J. Li, J. Guo, L.R. Yang, J. Fluoresc. 22 (2012) 201–212.
[22] A.A. Khandar, K. Nejati, Polyhedron 19 (2000) 607–613.
[23] S. Susan, F. Fatemeh, A.E. Abbas, H. Naeimi, Sens. Actuat. B 114 (2006) 928–935.